ORIGINAL PAPER

CrossMark

Electro-optical properties of poly(*N*-vinyl carbazole) nanoclay composites

Esma Ahlatcıoğlu Özerol[1]

Abstract

In this work, different weight percentages of nanoclay (NC) (2% and 5%) and *N*-vinyl carbazole were prepared by chemical polymerization. For investigation of structure, optical and morphologies of samples, Fourier transform infrared spectroscopy, ultraviolet–visible spectroscopy and scanning electron microscopy were used, respectively. Moreover, dielectric properties of composites were examined using dielectric analysis system and vector network analyzer system at high frequency. It was seen that the values of the real and imaginary dielectric constants and loss factor decrease with doping nanoclay into poly(*N*-vinyl carbazole) (PNVC). The conductivity properties of all samples were studied, and "*s*" parameter was calculated. Up to 1.7 GHz, "*s*" parameter value correlated with Jonscher power law, and between 1.7 GHz and 20 GHz, "*s*" parameter value correlated with superlinear power law. Also, the atomic polarization behaviors in the high-frequency regions have been obtained for PNVC and PNVC doped with 2%, 5% NCs at 25 °C.

Keywords Poly(*N*-vinyl carbazole) · Nanoclay · Composite · Conducting polymer · Dielectric

Introduction

Conducting polymers are attractive materials due to remarkable properties such as their simple synthesis, good environmental stability and electrical conductivity [1–3]. On the other hand, conducting polymers have some handicaps in their processing aspect because of insoluble, poor mechanical properties [1, 4, 5].

The formation of composites is one of the most useful ways in order to overcome these limitations [1, 2, 6–8]. Thus, physical, optical and mechanical properties of a polymer can be controlled and enhanced. The researchers synthesize

✉ Esma Ahlatcıoğlu Özerol
   eahlatci@yildiz.edu.tr

[1] Department of Bioengineering, Yıldız Technical University, Istanbul, Turkey

conducting polymer composites used to enhance the mechanical, physical and optical properties of conducting polymers [9, 10].

Conductive polymer nanocomposites have a remarkable feature in nanoscience and technology because of improvement in the mechanical, electrical and thermal properties of polymers [11–16].

Poly(vinyl carbazole) (PVC) is the oldest known (since 1957) [17] and most widely characterized polymeric photoconductor. Poly(N-vinyl carbazole) (PNVC) is a more attractive photoconductive polymer because of wide using applications such as photorefractive materials, polymeric light-emitting diodes and photovoltaic devices [18]. Since the first successful use of PNVC in electrophotographic applications [19, 20], polymers with carbazole moieties have been often investigated. PNVC was used as a dielectric and heat-resistive material but these days it is used also in photoconductive material [21, 22].

Synthesized polymeric clay nanocomposites are widely used because of their unique properties such as availability, good swelling properties and low cost [23]. The application areas of the clay nanocomposites are optoelectronics devices, sensors, rechargeable batteries, etc. [23].

In this work, different weight percentages of nanoclay (NC) (2% and 5%) and N-vinyl carbazole were prepared by chemical polymerization. The polymerization was performed by using AIBN (azobisisobutyronitrile) as an initiator at 70 °C during 24 h. The obtained composites were characterized by spectroscopic, morphological, optical and dielectric measurements at high frequency.

In difference to the earlier works, this study provides a detailed investigation of the dielectric properties at high frequencies and spectroscopic and morphological characterization of PNVC–NC composites. PNVC–NC composites have been synthesized for the first time in this study. The novelty of this work is investigation of changes in dielectric parameters at high frequencies by doping nanoclay in nanoscale. It could be important for miscellaneous technological uses areas such as commercial and military area because the electromagnetic wave in the GHz ranges has been widely applied in wireless telecommunication systems area, radar and local area network, etc. [24].

Experimental part

Materials and instruments

N-Vinyl carbazole (Aldrich), azobisisobutyronitrile (AIBN) (Aldrich), nanoclay (Aldrich) and all the other chemicals used were of analytical grade and were used as received without any further purification. The samples have been characterized by SEM (Jeol 7001F), FTIR (Nicholet), UV–VIS–NIR (Shimadzu 3600) spectrophotometer, and dielectric analysis system (Fytronix FY-3000) and Vector Network Analyzer (Anritsu) in the frequency range of 200 MHz–20 GHz.

Preparation of PNVC and its composites

In this study, different weight percentages of nanoclay (2% and 5%) were used. NVC was placed into 20 mL of NMP and was sonicated 25 °C, and then radical polymerization of NVC was performed by using AIBN in the presence of clay at 70 °C. Because of removal of some soluble monomer and initiator contaminants, the mixture was transferred into ethanol. After that, the samples were dried under vacuum at 25 °C for 24 h.

Results and discussion

Spectroscopic characterization

The FTIR spectra of the homopolymer PNVC and its polymer composites PNVC + 2%NC and PNVC + 5%NC in powder form are shown in Fig. 1. The characteristic peaks observed for PNVC were ring deformation of the substituted aromatic structure at 719 cm^{-1}, –CH$_2$ rocking vibrations at 745 cm^{-1}, out-of plane deformation of the vinylidene group at 1220 cm^{-1}, –CH$_2$ deformation of the vinylidene group at 1330 cm^{-1}, ring vibrations of the *N*-vinyl carbazole moiety at 1450 cm^{-1}, C=C stretching vibrations of the vinylidene group at 1680 cm^{-1} and aromatic C–H stretching vibrations at 3050 cm^{-1}. These results suggest that PNVC was formed and convenient with the literature [25].

In addition of the PNVC composites, the Si–O–Si stretching frequency bond was formed in addition of clay at about 1027 cm^{-1} [26, 27].
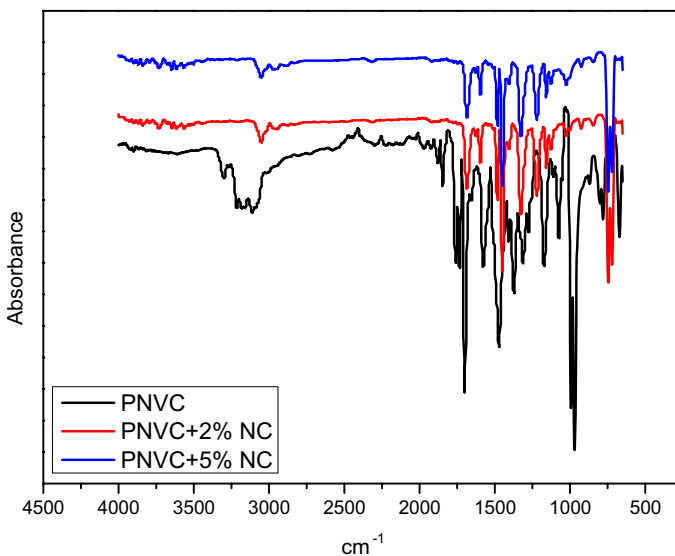

Fig. 1 FTIR spectra of PNVC, PNVC + 2% NC and PNVC + 5% NC

Figure 2 shows that plot of $(\alpha h\nu)^2$ plotted versus photon energy ($h\nu$) of PNVC, PNVC + 2% NC and PNVC + 5% NC. The energy band gap value for PNVC and its composites was calculated by UV–Vis spectra. The band gap value decreases with increase of nanoclay due to the homogeneous structure of the nanoclay.

Morphological characterization

Morphological characterization of PNVC samples was carried out by scanning electron microscopy (SEM). The SEM pictures of PNVC (Fig. 3a) and PNVC composites (PNVC + 2%NC and PNVC + 5%NC) are shown in Fig. 3b, c, respectively. As can be seen in Fig. 3a, the various shapes were seen for the PNVC morphology [28] and the NC in different percentages was attached with PNVC (Fig. 3a, b). It is seen that the NC particles are fairly well dispersed in the PNVC matrix and layered structure is formed by the addition of nanoclay (Fig. 3c).

The TEM figure (Fig. 4) shows the structure of clay which is convenient to the literature. There is a homogenous distribution of the clay flakes [29].

Dielectric properties

For dielectric characterization, the samples were prepared in the form of pellets under 10 ton cm^{-2} pressure forming a circular disk with dimensions 13 mm in diameter and 1 mm in thickness. The samples were measured by vector network analyzer (VNA) by using coaxial cable method. The dielectric constant was estimated by Fytronix FY-3000 dielectric analyzer system in the frequency range of 200 MHz–20 GHz, and the measurement was made in this frequency range [30].
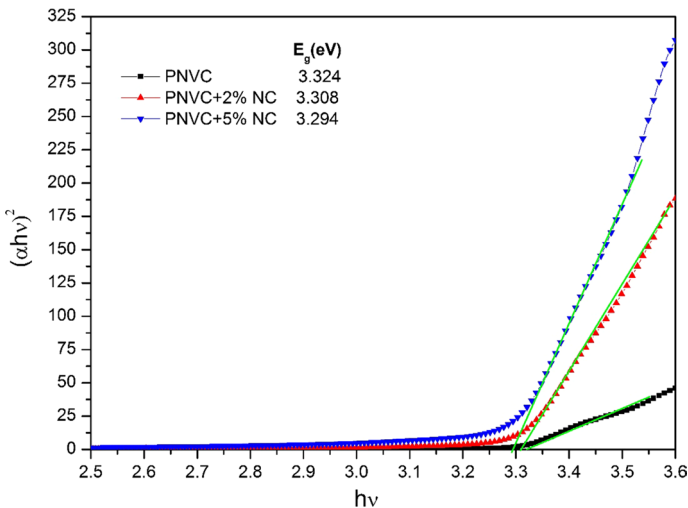
Fig. 2 Evolution of $(\alpha h\nu)^2$ plotted versus photon energy ($h\nu$) of the PNVC and PNVC with different nanoclay concentrations and the energy band gap value of samples
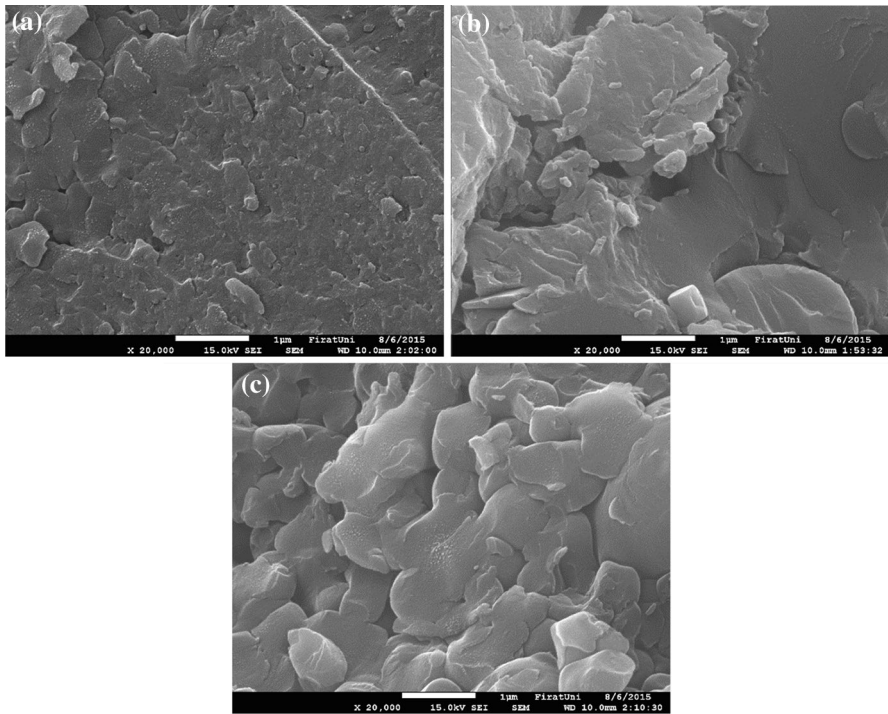
Fig. 3 SEM picture of PNVC (**a**) and PNVC doped with 2% (**b**), 5% NC (**c**), respectively
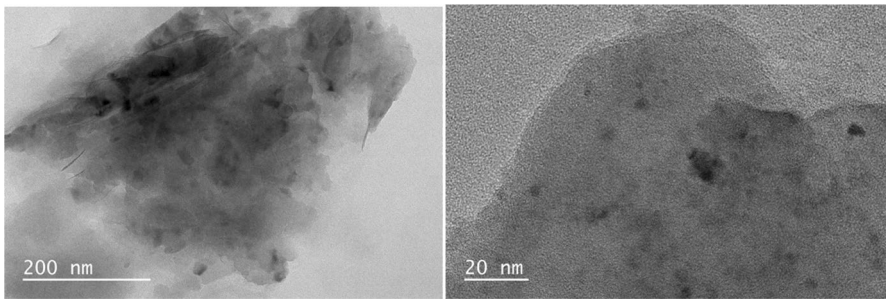
Fig. 4 TEM picture of NC with different magnifications

ε^* is the complex dielectric constant. The complex dielectric constant values were measured by VNA systems.

ε^* consists of the real ε' and imaginary ε'' components, which represent the stored and dissipated energy components of the material, respectively [31]:

$$\varepsilon^*(\omega) = \varepsilon'(\omega) + \varepsilon''(\omega) \tag{1}$$

Angular frequency ω is referred to by the radial frequency, $\omega = 2\pi f$, where f is the frequency [32, 33].

The loss tangent tan δ is defined as the ratio of the imaginary part to the real part of dielectric constant.

$$\varepsilon'' = \varepsilon' \cdot \tan \delta \qquad (2)$$

Dielectric parameters (ε', ε'', tanδ) and AC conductivity (σ) were measured at high frequencies. Initially, the real part of the dielectric constant showed an increase due to atomic interaction. As the frequency increased, the real (ε') part of dielectric constant decreased up to the critical frequency which is approximately 2.75 GHz and then minimum energy storage increases with increase of frequency. After 4 GHz, the real part of dielectric constant decreases with increase of frequency. PNVC and PNVC + 5% have highest and lowest values of the real (ε') part of dielectric constant (Fig. 5), respectively. As can be seen from this, the real (ε') part of dielectric constant was decreased by adding nanoclay.

Firstly, the imaginary part of dielectric constant decreases with increase of frequency up to 2 GHz. After 2 GHz, the dielectric constant increases up to approximately 2.75 GHz which is a critical frequency. After 4 GHz, the imaginary part of dielectric constant increases with increase of frequency. PNVC and PNVC + 5% have highest and lowest values of the imaginary (ε'') part of dielectric constant (Fig. 6), respectively. The atomic polarization behaviors in the high-frequency regions have been obtained for PNVC and PNVC doped with 2%, 5% NCs at 25 °C.

The energy loss decreases up to 2 GHz. After critical frequency (approximately 2.75 GHz), the loss factor increases with increase of frequency. PNVC has high value of loss factor at high frequency, but adding nanoclay to PNVC, the loss factor decreases (Fig. 7). The minimum value of energy loss has reached around the critical frequency.
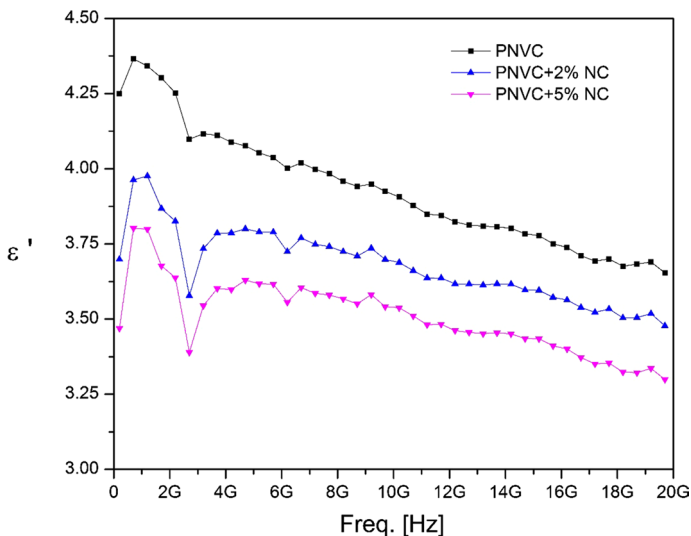
Fig. 5 Frequency evolution of the real (ε') part of dielectric constant for PNVC and PNVC with different NC concentrations
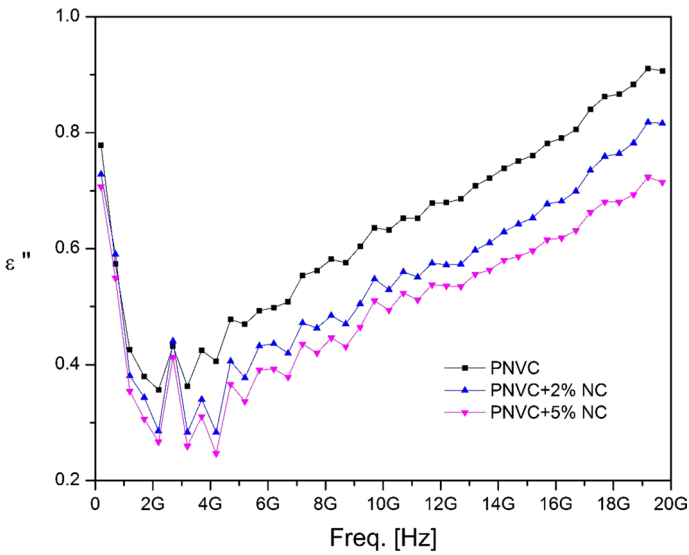
Fig. 6 Frequency evolution of the imaginary (ε'') part of dielectric constant for PNVC and PNVC with different NC concentrations
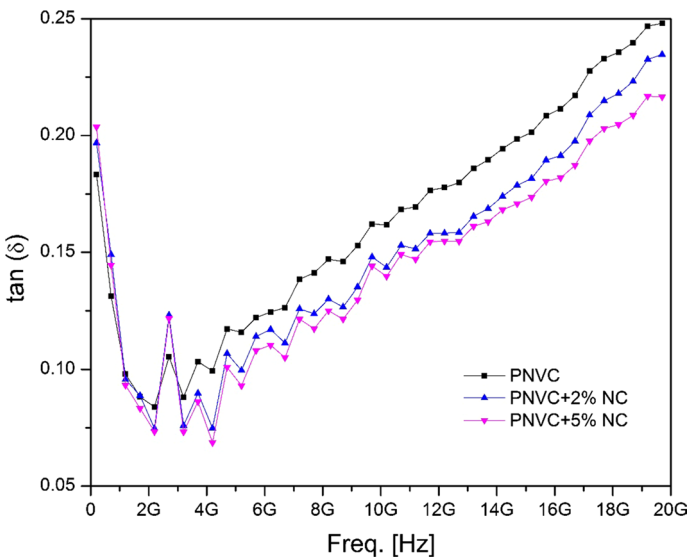
Fig. 7 Frequency variation of the loss factor for PNVC and PNVC with different NC concentrations

The AC conductivity value increases with increase of frequency in order of PNVC and PNVC with different NC concentrations as shown in Fig. 8. The AC conductivity exhibits increasing trends with frequency. PNVC has highest value of conductivity. Because of oxidation effect, the conductivity value decreases
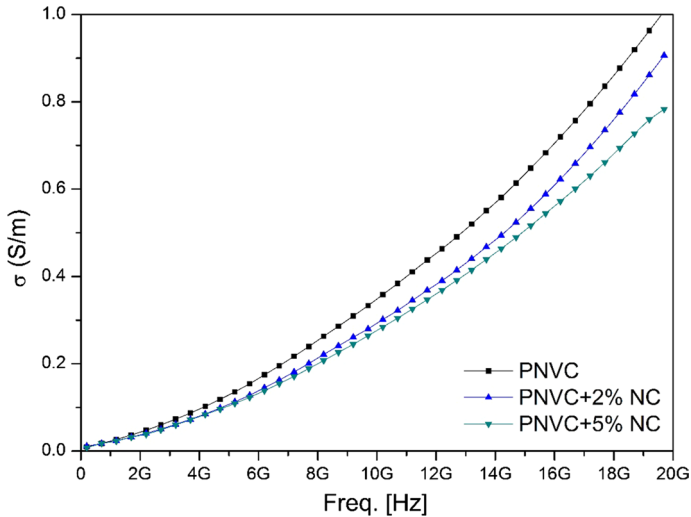
Fig. 8 Frequency variation of the conductivity for PNVC and PNVC with different NC concentrations

with adding nanoclay to PNVC. The conductivity values decrease with frequency due to the low mobility of nanoclay. The conductivity properties of NC-doped PNVC are changed with the nanosize of nanoclay particles.

The AC conductivity dependence of frequency can be expressed as the empirical Jonscher's universal law [32] because of determination of AC conduction mechanism:

$$\sigma_{AC}(\omega) = A\omega^s, \tag{3}$$

where A is a constant, ω is the angular frequency and s is the frequency exponent parameter.

The angular frequency exponent value s was calculated from the slopes of Fig. 9 [34]. The $\ln(\sigma_{AC})$ versus ω plot is given in Fig. 9 for all samples. From the slopes two range of Fig. 9 for the first region and second frequency regions (Table 1), the angular frequency exponent values s can be calculated [34] because the frequency exponent is used to determine the electrical conduction mechanism of all samples. Frequency exponent "s" was restricted to be $0 < s < 1$ which is known as Jonscher power law (JPL). JPL is proposed to exist at mega- to 3 GHz frequency range in the first region. The another power law for frequency-dependent conductivity is superlinear power law (SLPL) which is related to frequency exponent between one and two [35]. However, for PNVC and PNVC doped with nanoclays, the AC conductivity mechanism is in agreement with SLPL at the 3G to 18G Hz frequency (II. Region).
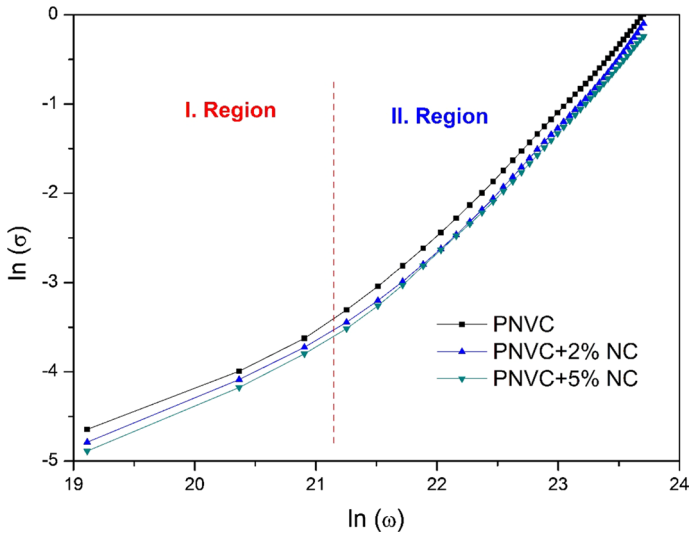
Fig. 9 AC conductivity for PNVC and PNVC with different NC concentrations

Table 1 S parameters of the samples

Samples	I. Region	II. Region
PVNC	0.56	1.39
PVNC+2%NC	0.58	1.40
PVNC+5%NC	0.60	1.37

Conclusion

In this work, PNVC/NC powder composites have been synthesized by chemical polymerization of *N*-vinyl carbazole in the presence of different weight percentages of nanoclay powder and AIBN as initiator at 70 °C for 24 h.

PNVC and PNVC with different NC concentrations have been investigated by chemical and morphological characterization using the FTIR and SEM, respectively. Frequency evolution of the real (ε') and (ε'') parts of dielectric constant, loss factor, AC conductivity behavior for PNVC and its composites have been determined by the impedance spectroscopy at room temperature.

Depending on the nanoclay doping, more compact materials were obtained. It has also been seen in SEM that the spacing is reduced with the addition of nanoclay. It was observed that the obtained composites by doping of nanoclay were contributed to the change in the conductivity values with increasing frequency.

All the samples show the atomic polarization behavior in the high-frequency regions at 25 °C.

PNVC and PNVC doped with nanoclays correspond to the AC conductivity behavior which is in agreement with JPL and SLPL at the first and second frequency regions, respectively.

References

1. Khatoon H, Ahmad S (2017) A review on conducting polymer reinforced polyurethane composites. J Ind Eng Chem 53:1–22
2. Sethi D, Ram R, Khastgir D (2017) Electrical conductivity and dynamic mechanical properties of silicon rubber-based conducting composites: effect of cyclic deformation, pressure and temperature. Polym Int 66(9):1295–1305
3. Sethi D, Ram R, Khastgir D (2018) Analysis of electrical and dynamic mechanical response of conductive elastomeric composites subjected to cyclic deformations and temperature. Polym Compos 39(11):3912–3923
4. Vicentini DS, Barra GM, Bertolino JR, Pires AT (2007) Polyaniline/thermoplastic polyurethane blends: preparation and evaluation of electrical conductivity. Eur Polym J 43(10):4565–4572
5. Subramaniam CK, Kaiser AB, Gilberd PW, Liu CJ, Wessling B (1996) Conductivity and thermopower of blends of polyaniline with insulating polymers (PETG and PMMA). Solid State Commun 97(3):235–238
6. Ram R, Rahaman M, Khastgir D (2014) Mechanical, electrical, and dielectric properties of polyvinylidene fluoride/short carbon fiber composites with low-electrical percolation threshold. J Appl Polym Sci 131(3):39866
7. Ram R, Rahaman M, Aldalbahi A, Khastgir D (2017) Determination of percolation threshold and electrical conductivity of polyvinylidene fluoride (PVDF)/short carbon fiber (SCF) composites: effect of SCF aspect ratio. Polym Int 66(4):573–582
8. Snook GA, Bhatt AI, Abdelhamid ME, Best AS (2012) Role of H+ in polypyrrole and poly(3, 4-ethylenedioxythiophene) formation using $FeCl_3 \cdot 6H_2O$ in the room temperature ionic liquid, C4mpyrTFSI. Aust J Chem 65(11):1513–1522
9. Ram R, Khastgir D, Rahaman M (2018) Physical properties of polyvinylidene fluoride/multi-walled carbon nanotube nanocomposites with special reference to electromagnetic interference shielding effectiveness. Adv Polym Technol
10. Ram R, Rahaman M, Khastgir D (2015) Electrical properties of polyvinylidene fluoride (PVDF)/multi-walled carbon nanotube (MWCNT) semi-transparent composites: modelling of DC conductivity. Compos A Appl Sci Manuf 69:30–39
11. Rahman MS, Hammed WA, Ro Y, Ekramul Mahmud HNME (2017) Optoelectrical and photoluminescence quenching properties of poly(N-vinyl carbazole)-polypyrrole/reduced graphene oxide nanocomposites. Synth Met 226:188–194
12. Zhong J, Gao S, Xue G, Wang B (2015) Study on enhancement mechanism of conductivity induced by graphene oxide for polypyrrole nanocomposites. Macromolecules 48:1592–1597
13. Yoon H (2013) Current trends in sensors based on conducting polymer nanomaterials. Nanomaterials 3:524–549
14. Lei W, Si W, Xu Y, Gu Z, Hao Q (2014) Conducting polymer composites with graphene for use in chemical sensors and biosensors. Microchim Acta 181:707–722
15. Yoo D, Kim J, Kim JH (2014) Direct synthesis of highly conductive poly(3,4-ethylenedioxythiophene): poly(4-styrenesulfonate)(PEDOT:PSS)/graphene composites and their applications in energy harvesting systems. Nano Res 7:717–730
16. Ravindranadh K, Rao MC (2013) Physical properties and applications of conducting polymers: an overview. Int J Adv Pahrm Biol Chem 2:190–200
17. Grund S, Eichberg J, Asmussen F (1982) A specific embedding resin (PVK) for fine cytological investigations in the photoemission electron microscope. J Ultrastruct Res 80:89–97
18. Huang CF, Hsieh YA, Hsu SC, Matyjaszewski K (2014) Synthesis of poly(N-vinyl carbazole)-based block copolymers by sequential polymerizations of RAFT-ATRP. Polymer 55:6051–6057
19. Grazulevicius JV, Strohriegl P, Pielichowski J, Pielichowski K (2003) Carbazole-containing polymers: synthesis, properties and applications. Prog Polym Sci 28:1297–1353

20. Petukhova A, Greener J, Liu K, Nykypanchuk D, Nicolay R, Matyjaszewski K, Kumacheva E (2012) Standing arrays of gold nanorods end-tethered with polymer ligands. Small 8:731–737

21. Block H, Bowker SM, Walker SM (1978) Photoconductivities of poly(N-vinyl carbazoles) containing cation radicals. Polymer 19:531–536

22. Penwell RC, Prest WM Jr (1978) Orientation in poly(n-vinyl carbazole) by melt extrusion. Polymer 19:537–541

23. Ahlatcıoğlu E, Şenkal BF, Okutan M (2015) Preparation and electrical characterization of poly(aniline) nano clay composites. High Temp Mater Process (London) 34:341–346

24. Aal NA, Al-Hazmi F, Al-Ghamdi AA, Al-Ghamdi AA, El-Tantawy F, Yakuphanoglu F (2015) A novel facile synthesis and electromagnetic wave shielding effectiveness at microwave frequency of graphene oxide paper. Microsyst Technol 21(10):2155–2163

25. Basavaraja C, Thinh PX, Huh DS (2013) Characterization and electrical behavior of biodegradable poly(n-vinylcarbazole)/poly(3-hydroxybutyric acid) composite films. Macromol Res 21:574–581

26. Mansour N, Momeni A, Karimzadeh R, Amini M (2012) Blue-green luminescent silicon nanocrystals fabricated by nanosecond pulsed laser ablation in dimethyl sulfoxide. Opt Mater Express 2:740–748

27. Lin SW, Chen DH (2009) Synthesis of water-soluble blue photoluminescent silicon nanocrystals with oxide surface passivation. Small 5:72–76

28. Boddula R, Srinivasan P (2014) Benzoyl peroxide oxidation route to the synthesis of solvent soluble polycarbazole. Int Sch Res Not 2014:1–9

29. Azzam EMS, Sayyah SM, Taha AS (2013) Fabrication and characterization of nanoclay composites using synthesized polymeric thiol surfactants assembled on gold nanoparticles. Egypt J Petrol 22(4):493–499

30. Yakuphanoglu F, Al-Ghamdi AA, El-Tantawy F (2015) Electromagnetic interference shielding properties of nanocomposites for commercial electronic devices. Microsyst Technol 21(11):2397–2405

31. Korkmaz B, Özerol EA, Bozdoğan AÇ, Okutan M, Şenkal BF, Gursel YH (2017) Synthesis and characterization of a new hydrogen bonded side chain liquid crystal block copolymer and investigation of electrical properties. Pure Appl Chem 89(1):19–28

32. Ahlatcıoğlu E, Gursel Y, Okutan M, Senkal BF (2014) Preparation of poly (N-vinylcarbazole)-co-poly (2-(dimethylamino) ethyl methacrylate) based hydrogen bonded side-chain liquid crystal copolymer. Mater Sci Semicond Process 28:144–150

33. Jonscher AK (1978) The universal dielectric response: a review of data their new interpretation. Chelsea Dielectrics Group, London

34. Ahlatcıoğlu Özerol E, Şenkal BF, Okutan M (2015) Preparation and characterization of graphite composites of polyaniline. Microelectron Eng 146:76–80

35. Meller A (1983) Gmelin Handbuch der Anorganische Chemie, Boron compounds, 2nd edn. Springer, Berlin